Fluctuation and Transport Reduction in a Reversed Field Pinch by Inductive Poloidal Current Drive

J. S. Sarff, S. A. Hokin, H. Ji, S. C. Prager, and C. R. Sovinec
University of Wisconsin, Madison, Wisconsin 53706
(Received 23 December 1993)

An auxiliary poloidal inductive electric field applied to a reversed field pinch plasma reduces the current density gradient, slows the growth of $m=1$ tearing fluctuations, suppresses their associated sawteeth, and doubles the energy confinement time. Small sawteeth occur in the improved state but with $m=0$ precursors. By requiring a change of toroidal flux embedding the plasma, inductive poloidal current profile drive is transient, but the improvement encourages the program of reversed field pinch transport suppression using current profile control.

PACS numbers: 52.55.Hc, 52.25.Fi, 52.25.Gj, 52.35.Py

The search for solutions to the problem of fluctuation-induced transport in magnetically confined plasmas absorbs the efforts of many plasma researchers. Proposed strategies based on notions of plasma behavior are often tested, but improved confinement usually results unexpectedly. In the case of the reversed field pinch (RFP), magnetic-fluctuation-induced transport dominates other loss mechanisms. The fluctuation amplitude is typically 1% of the mean field [1], and the estimated energy loss by stochastic magnetic field diffusion [2] easily accounts for the observed global energy flux [3]. Recent measurements of the magnetic-fluctuation-induced electron energy flux in the Madison Symmetric Torus (MST) directly identify large transport associated with the magnetic fluctuation [4], supporting the long-standing view that closed magnetic flux surfaces are absent in the core of the RFP.

More than 90% of the RFP magnetic fluctuation results from several poloidal mode number $m=1$, toroidal mode number $n\sim 2R/a$ core-resonant tearing (or resistive kink) instabilities. The close spatial proximity of their resonant magnetic surfaces encourages magnetic island overlap and stochasticity. An understanding of these magnetohydrodynamics fluctuations [5], which correlate with the energy transport, led researchers to propose methods for their elimination. Tearing fluctuation stems from the current density gradient, so the proposals employ electrostatic [6] or rf [7,8] poloidal current drive in the outer region of the plasma, eliminating the need for fluctuation-dynamo sustainment of the RFP.

In this Letter we describe the first observation of reduced transport resulting from current profile control in an RFP. We call this experiment pulsed poloidal current drive (PPCD) as it uses inductive methodology. Unlike electrostatic or rf current drive, PPCD is transient since it requires a change of toroidal flux embedding the plasma. PPCD exemplifies a rare and successful progression from the identification of destructive turbulence to a theoretical understanding which motivates a corrective measure.

The PPCD experiment is performed in MST [9], a large reversed field pinch with major radius $R=1.5$ m, minor radius $a=0.52$ m, toroidal plasma current $I_\phi \leq 700$ kA, and poloidal beta $\beta_\theta \sim 10\%$. Figure 1 summarizes a PPCD experiment in which a small high voltage capacitor bank drives a fast current pulse in the toroidal field winding to induce a poloidal electric field E_θ. The pulse is initiated at $t=12$ ms, marked by the vertical dashed lines. The one-turn poloidal V_θ and toroidal V_ϕ surface voltages shown in Fig. 1(a) generate the poloidal I_θ and toroidal I_ϕ plasma currents shown in Fig. 1(b), although strong coupling prevents identifying V_θ only with I_θ and vice versa. To direct E_θ for current profile flattening, the volume average toroidal field $\langle B_\phi \rangle$ and the toroidal field at the wall $B_{\phi w}$ must decrease as in Fig. 1(c). PPCD increases $I_\theta = 2\pi R(B_0 - B_{\phi w})/\mu_0$, the poloidal plasma current between the magnetic axis and plasma edge which is inferred from $\oint \mathbf{B}\cdot d\boldsymbol{l}$ on the magnetic axis. (The axis magnetic field B_0 is estimated using an RFP equilibrium model [10].) Note that V_θ is nonzero as I_ϕ increases since toroidal flux is generated by dynamo action. The Fig. 1 data are averages for eleven PPCD plasmas.

Since tearing instability results from the gradient in $J_\parallel/B$ we fit the experiment by the three parameter equilibrium model [11]

$$\nabla\times\mathbf{B}=\lambda_0(1-r^\alpha)\mathbf{B}+(\beta_0/2B^2)\mathbf{B}\times\nabla p \qquad (1)$$

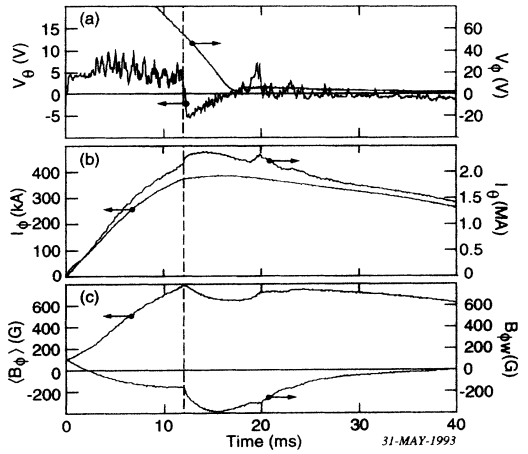

FIG. 1. Shot-averaged wave forms of (a) the surface voltages, (b) the plasma current, and (c) the average and wall toroidal field.

0031-9007/94/72(23)/3670(4)$06.00

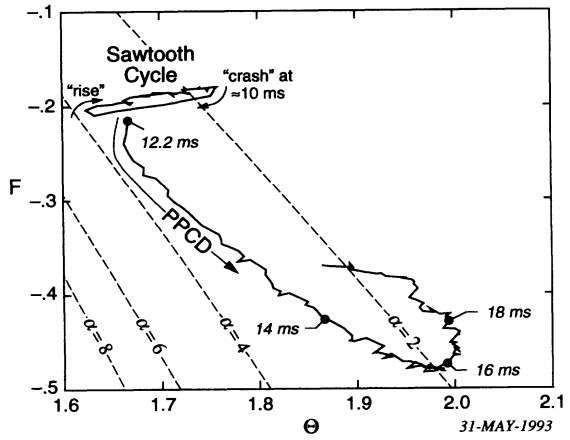

FIG. 2. Shot-averaged F-Θ trajectories during PPCD and a sawtooth oscillation.

to estimate the shape of the (normalized) parallel current profile $\lambda(r)=\mu_0 a\mathbf{J}\cdot\mathbf{B}/B^2$. Large α corresponds to a flat parallel current density profile. $\beta_0=2\mu_0 p_0/B_0^2$ is the central beta value, and the pressure profile is assumed quadratic $p(r)=1-r^2$. In general, the perpendicular current details weakly affect the parallel current fit.

PPCD flattens the current profile in degree comparable to a sawtooth oscillation "crash" [12]. This comparison benchmarks PPCD since in a sawtooth crash the plasma self-flattens its unstable current profile. To illustrate, we plot the F-Θ trajectory where F is the cylindrical reversal parameter, $F\equiv B_{\phi w}/\langle B_\phi\rangle$, and Θ is the cylindrical pinch parameter, $\Theta\equiv B_{\theta w}/\langle B_\phi\rangle$. $B_{\theta w}$ and $B_{\phi w}$ are the poloidal and toroidal magnetic fields at the plasma surface, respectively. (F and Θ are alternate parameters to λ_0 and α.) The PPCD F-Θ trajectory is shown in Fig. 2 for $12.2\le t\le 19.5$ ms data in Fig. 1. Solutions to Eq. (1) for $\beta_\theta=2\mu_0\langle p\rangle/B_{\theta w}^2=10\%$ are indicated by the dashed contours of constant α. For comparison, the average F-Θ trajectory of the sawtooth oscillation which crashed at $t\approx 10$ ms in the eleven PPCD discharges is also shown in Fig. 2. The PPCD phase gradually terminates as the current profile again peaks and becomes sawtooth unstable when $\alpha\lesssim 2$. A series of unusually large sawteeth starting around $t\approx 18$ ms cause the plasma to relax toward normal RFP equilibria.

By flattening the current profile, PPCD slows the growth of $m=1$ fluctuations and suppresses their associated sawteeth. Magnetic fluctuations are measured in MST with arrays of magnetic pickup sensors (B_θ, B_ϕ, B_r) attached to the inner vacuum vessel surface. In this work, toroidal mode $n\le 15$ spectra are derived from 32 equally spaced magnetic pickup sensors. The most active modes in a typical n spectrum of $\tilde{B}_\theta$ from a single PPCD plasma are shown in Fig. 3. Before the application of the pulse, the spectrum exhibits the usual precursory growth of the $n=5$–10, $m=1$ modes associated with the sawtooth cycle. When PPCD is applied, their growth is

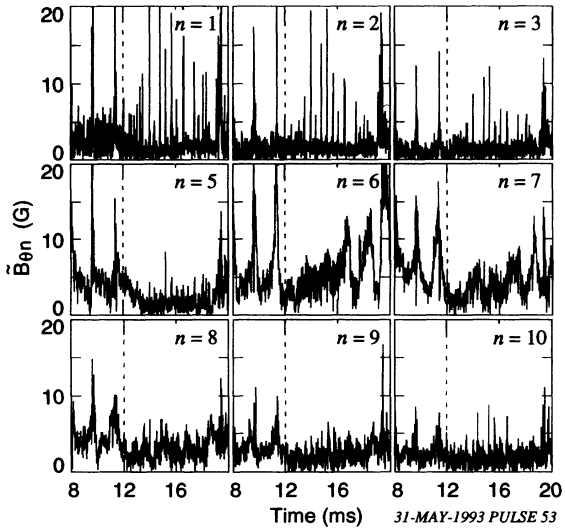

FIG. 3. Dominant modes of a single shot $\tilde{B}_\theta$ toroidal n spectrum during PPCD.

dramatically slowed. The spatial root-mean-square (rms) fluctuation amplitude $\tilde{B}_{\theta\,\mathrm{rms}}=\sqrt{\sum_n b_{\theta n}^2}$ for $n\le 15$ is shown in Fig. 4(a). The maximum amplitude is about 3 times the minimum amplitude between sawtooth crash events; PPCD maintains this minimum value for several milliseconds. The lack of sawtoothing decreases the average fluctuation amplitude by 25% during PPCD, observable in the (time-smoothed) plot of the eleven-shot-average rms fluctuation overlaying the single shot record in Fig. 4(a).

Although PPCD eliminates sawteeth preceded by the $m=1$ fluctuation, different sawteeth occur during PPCD. Like conventional sawteeth, they correlate with decreases in the soft x-ray flux [Fig. 4(b)] and increases in toroidal flux, but the amplitude changes are small. The n spectra reveal increased precursory activity in the $n=1$–3 modes, not in the band $n=5$–10. This activity, if resonant, corresponds to the $m=0$ fluctuation since the safety factor

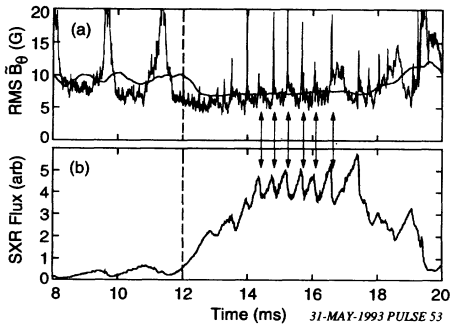

FIG. 4. (a) The spatial rms fluctuation in $\tilde{B}_\theta$ for the spectrum in Fig. 3. The smooth curve is the shot-averaged rms fluctuation. (b) Central-chord soft x-ray emission. Arrows mark small sawteeth during PPCD.

satisfies $|q(r)| \lesssim \frac{1}{5}$, even during PPCD. Simultaneous spectral measurements of both $\tilde{B}_\phi$ and $\tilde{B}_\theta$ show $\tilde{B}_\phi/\tilde{B}_\theta \gtrsim 5$, consistent only with $m=0$ instability since the sensors are located in a current-free region [13]. In addition to sawtoothing, the low n mode amplitudes steadily grow to precrash values when PPCD is increased to the level where $\langle B_\phi \rangle$ is halved by the pulse. In moderate amplitude PPCD, the steady $m=0$ growth is avoided. Interestingly, numerical modeling of the PPCD experiment using the three-dimensional (cylindrical), nonlinear, resistive MHD, initial value code DEBS [14] predicts reduced, not stabilized, $m=1$ fluctuation. However, it fails to predict enhanced $m=0$ fluctuation.

PPCD doubles the energy confinement by halving the Ohmic input power while slightly increasing the stored thermal energy. The solid curves in Fig. 5 show shot-averaged wave forms of the central chord electron density n_e, the charge-exchange ion temperature T_i, P_{Ohmic} (E_θ included), and the total radiated power P_{rad} (bolometrically measured) for the eleven PPCD plasmas. Also shown are soft x-ray, H_α, and near-infrared bremsstrahlung ($\propto n^2 Z_{\text{eff}}/\sqrt{T_e}$) radiation measurements. The dashed line wave forms are for a set of eight discharges with PPCD turned off. These were operated identically to PPCD except a small gas puff was injected at $t=10$ ms to mimic a modest density increase during PPCD. The electron temperature T_e is estimated from a self-consistent analysis of the density n_e, Si(Li) detector x-ray energy spectra, and two different thickness beryllium foil filtered x-ray measurements. At $t=17$ ms, $T_e \approx 250$ eV with PPCD and $T_e \approx 200$ eV without PPCD; the latter is consistent with the most recent database of MST Thomson scattering data [15]. (The MST Thomson scattering diagnostic was inoperable during this PPCD experiment.)

Assuming flat temperature and parabolic density profiles (consistent with the four interferometer chords inside $r/a=0.6$), the energy confinement time at $t=17$ ms is $\tau_E = 3\pi^2 a^2 R \langle n_e \rangle (T_e + T_i)/P_{\text{Ohmic}} \approx 1.0$ ms without PPCD and $\tau_E \approx 2.2$ ms with PPCD. In standard RFP operation, τ_E scaling [15] in MST is weakly dependent on I_ϕ and n_e, varying little about $\tau_E = 1$ ms. Because the stored magnetic energy changes during PPCD, the calculation of P_{Ohmic} was cross-checked using several equilibrium models [10,11,16]. The polynomial function model [10] calculation, shown in Fig. 5(c), gives slightly larger values for P_{Ohmic} than the other models.

The particle confinement time τ_p also increases during PPCD. This is indicated by the 40% decrease in H_α emission and moderate rise in n_e. Particle transport modeling estimates τ_p increased by a factor of about 1.7 during PPCD.

PPCD reduces the anomalous plasma resistance. The change in toroidal plasma resistance from increased poloidal field line twist during PPCD almost balances the change from reduced classical resistivity $\eta \propto Z_{\text{eff}}/T_e^{3/2}$. ($T_e$ increases, and Z_{eff} decreases by about 20%.) Therefore most of the reduction in P_{Ohmic} results from a 40% decrease in anomalous plasma resistance [17] during PPCD. This conclusion is sensitive to the error in the T_e measurement, but a 50% T_e increase or a dramatic T_e profile change is required to explain the P_{Ohmic} reduction classically. From the combined reductions in Z_{eff} and anomalous effects, the multiplier of the $Z=1$, flat temperature profile resistance decreases from 3 to 1.5. Typical of RFP plasmas, the ion temperature exceeds expectations for collisional heating by electrons. If the anomalous input power heats the ions, as often assumed, then the reduced anomalous resistance and unchanged ion temperature during PPCD imply much reduced ion thermal loss.

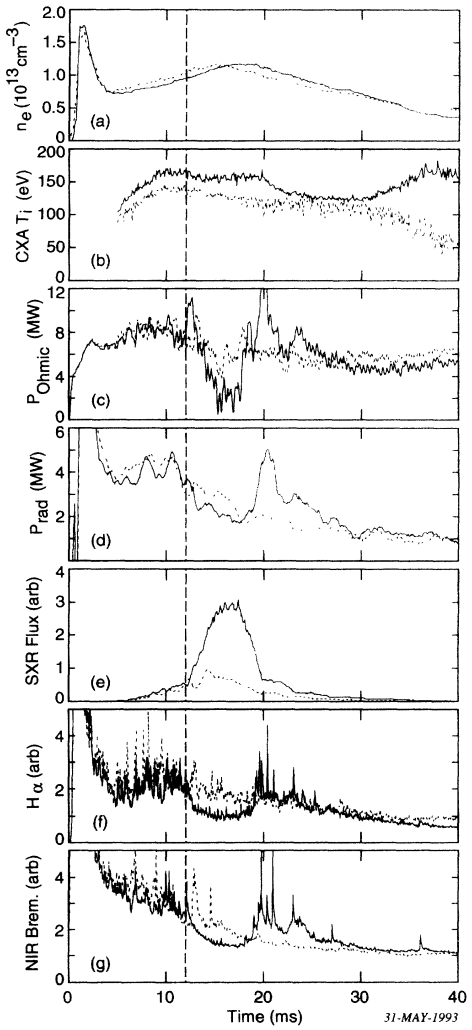

FIG. 5. Shot-averaged wave forms of (a) the central-chord line-averaged electron density, (b) the ion temperature, (c) the Ohmic input power, (d) the total radiated power, (e) soft x rays, (f) H_α emission, and (g) bremsstrahlung radiation with PPCD (solid curves) and without PPCD (dashed curves).

Improved confinement during PPCD depends on the

condition of the vacuum vessel wall. Clear improvement occurs with a boronized wall. (Solid target boronization is used in MST [18].) Without boronization, enhanced impurity influx coincides with the PPCD pulse. Even with boronization, if the pulse is applied well after current peak, impurity-injection-free PPCD is difficult to obtain.

In summary, inductive poloidal current drive flattens the current density profile, slows the growth of $m=1$ tearing fluctuations, suppresses their associated sawteeth, and doubles energy confinement. The particle confinement time also improves. A reduction in anomalous plasma resistance suggests PPCD reduces the dynamo effect. The improved plasma state exhibits small sawteeth, but they are preceded by $m=0$, $n\sim 1$ instability rather than $m=1$, $n\sim 6$ instability.

These results strongly encourage the program of the fluctuation and transport suppression using current profile control techniques in the RFP. Although the PPCD experiment falls short of the ultimate goal of eliminating tearing fluctuation, clear correlation exists between improved confinement, current profile flattening, and modest fluctuation suppression. If the transported energy loss scales like $\chi \propto \tilde{B}_r^2$, as expected for diffusion in a stochastic magnetic field [2], then the 25% reduction in the average fluctuation amplitude predicts a 45% reduction in energy transport. The observed doubling of the confinement time is consistent with this expectation, but the transported energy probably more than halved since the PPCD improved state has a higher fraction of radiated power. The plasma core could be on the verge of experiencing nonstochastic (closed) magnetic flux surfaces.

The authors are grateful for the assistance of the MST group, especially A. Almagri, M. Cekic, J. Frank, D. Den Hartog, J. Laufenberg, K. Mirus, D. Sinitsyn, W. Shen, and C. Sprott. We also acknowledge P. Figgliozi for computational assistance. This work was supported by the U.S. DOE.

[1] For example, V. Antoni and S. Ortolani, Plasma Phys. **25**, 799 (1983); D. Brotherton-Ratcliffe, C. G. Gimblett, and I. H. Hutchinson, Plasma Phys. Controlled Fusion **24**, 59 (1984); R. J. La Haye *et al.*, Phys. Fluids **27**, 2576 (1984); A. Almagri *et al.*, Phys. Fluids B **4**, 4080 (1992); P. R. Brunsell *et al.*, Phys. Fluids B **5**, 885 (1993).

[2] J. D. Callen, Phys. Rev. Lett. **39**, 1540 (1977); A. B. Rechester and M. N. Rosenbluth, Phys. Rev. Lett. **40**, 38 (1978).

[3] For example, I. H. Hutchinson *et al.*, Nucl. Fusion **24**, 59 (1984); K. Hattori *et al.*, Phys. Fluids B **3**, 3111 (1991).

[4] G. Fiksel, S. C. Prager, W. Shen, and M. Stoneking, Phys. Rev. Lett. **72**, 1028 (1994).

[5] Y. L. Ho and C. Craddock, Phys. Fluids B **3**, 721 (1991), and references therein.

[6] Y. L. Ho, Nucl. Fusion **31**, 341 (1991).

[7] S. Shiina *et al.*, in *Proceedings of the International School of Plasma Physics Workshop on the Physics of Alternative Magnetic Confinement Schemes,* Varenna, Italy (Societá Italiana di Fisica, Varenna, 1990), p. 903.

[8] E. Uchimoto *et al.*, Bull. Am. Phys. Soc. **38**, 1979 (1993).

[9] R. N. Dexter, D. W. Kerst, T. H. Lovell, S. C. Prager, and J. C. Sprott, Fusion Technol. **19**, 131 (1991).

[10] J. C. Sprott, Phys. Fluids **31**, 2266 (1988).

[11] V. Antoni *et al.*, Nucl. Fusion **26**, 1711 (1986).

[12] R. G. Watt and R. A. Nebel, Phys. Fluids **26**, 1168 (1983); S. Hokin *et al.*, Phys. Fluids B **3**, 2241 (1991).

[13] $i\mathbf{k}\times\mathbf{B}=0$ implies $nb_{\theta mn}/R = mb_{\phi mn}/a$ for each Fourier mode $\mathbf{b}_{mn}$. In a cylinder, $b_{\theta 0n}$ vanishes, but toroidal effects allow finite $b_{\theta 0n}$ for "$m=0$" instability.

[14] D. D. Schnack *et al.*, J. Comput. Phys. **70**, 330 (1987).

[15] S. Hokin *et al.*, in *Controlled Fusion and Plasma Physics,* Proceedings of the 20th European Conference, Lisbon, 1993 (European Physical Society, Petit-Lancy, 1993), Vol. II, p. 475.

[16] K. F. Schoenberg, R. F. Gribble, and J. A. Phillips, Nucl. Fusion **22**, 1433 (1982).

[17] Traditionally "anomalous" refers to $E_\parallel \neq \eta J_\parallel$ for classical η. This anomaly need not be mysterious given a dynamo electric field, e.g., $\langle \tilde{\mathbf{V}}\times\tilde{\mathbf{B}}\rangle_\parallel$.

[18] D. J. Den Hartog *et al.*, J. Nucl. Mater. **200**, 177 (1993).